

# Long-Term TRMM Data Improve Cloud Simulations

Xiaowen Li (612, GESTAR), Wei-Kuo Tao (612), Toshihisa Matsui (612, ESSIC)

Long-term satellite observations are very useful in validating and improving microphysical processes in a cloud-resolving model. We focus on ice-phase microphysics in the Goddard Cumulus Ensemble (GCE) model coupled to a Spectral Bin Microphysical Scheme and compare our simulations to surface and space-based radars. The spectral bin microphysical scheme explicitly simulates Particle Size Distributions (PSDs), thus avoiding a key weakness in more widely used bulk microphysical schemes, where PSDs have to be assumed.

- The initial **simulation over-estimated** radar reflectivity by more than 10 dBZ in the stratiform region, for both surface radar and space-borne TRMM Precipitation Radar. The simulated ice-phase particles are too large, especially between 4 km and 8 km.

- Several factors **may have contributed** to the over estimation of ice-phase reflectivity (too much ice in more reflective larger particles) : particle density, fall velocity, temperature dependency of particle collection efficiency, and the lack of spontaneous breakup in large particles.

- Introducing stronger temperature dependency collection efficiency has resulted** in the best agreement in magnitudes and characteristics of both radar CFADs and TMI brightness temperature distributions (third column in Figure 1).

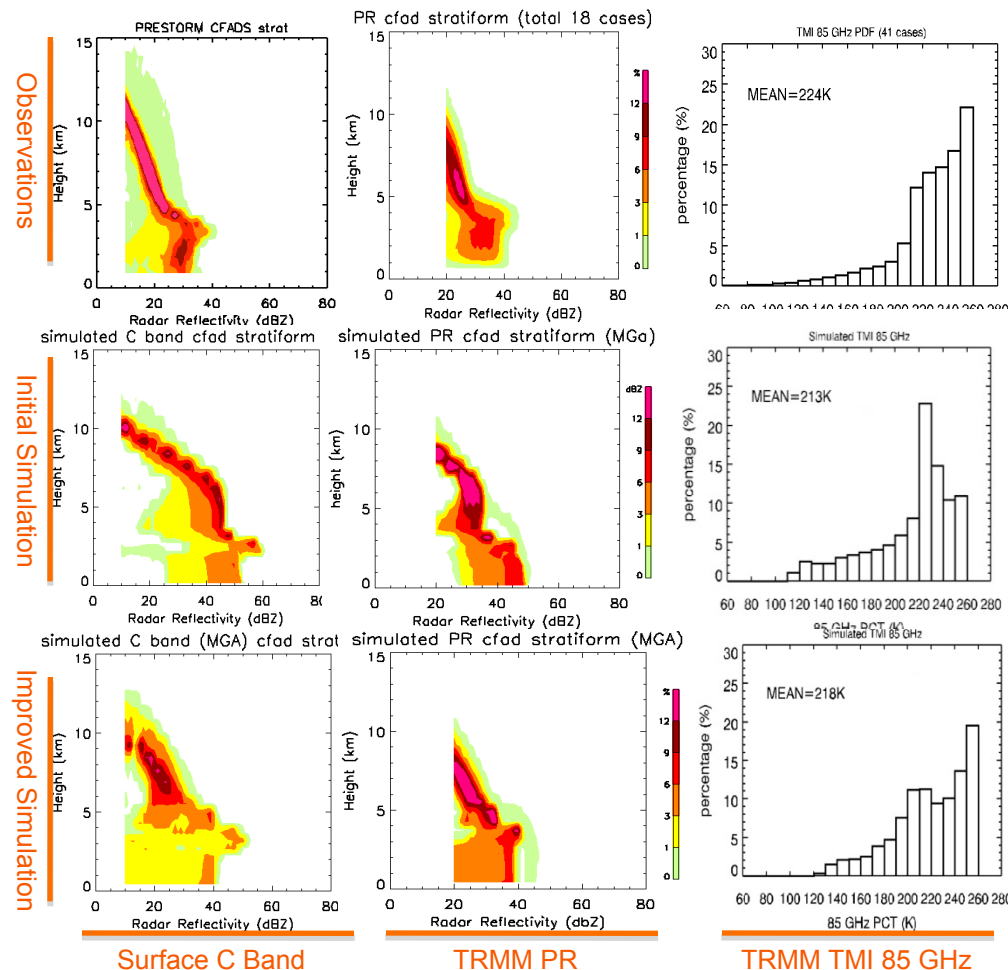


**Figure 1:** Comparisons of observations (first row), initial simulations (second row), and improved simulations (third row) of stratiform region in a mid-latitude squall line. The colour contours are radar reflectivity CFADs (Contoured Frequency by Altitude Diagrams). The first column is CFADs of surface-based C-Band Radar. The second column is composited from TRMM (Tropical Rainfall Measurement Mission) PR (Precipitation Radar). The third column is the frequency distributions of 85 GHz brightness temperature from TMI (TRMM Microwave Imager).



Name: Xiaowen Li, NASA GSFC, Code 612 and GESTAR, Morgan State University  
E-mail: Xiaowen.Li@nasa.gov  
Phone: 301-614-6319



#### References:

- Li, X, W.-K. Tao, T. Matsui, C. Liu, and H. Masunaga, 2010: Improving a spectral bin microphysical scheme using long-term TRMM satellite observations. *Quarterly Journal of Royal Meteorological Society*, **136**, 382-399.
- Li, X, W.-K. Tao, A. P. Khain, J. Simpson, D. E. Johnson, 2009: Sensitivity of a cloud-resolving model to bulk and explicit bin microphysical schemes. Part I: Comparisons. *Journal of Atmospheric Sciences*, **66**, 3-21.
- Li, X, W.-K. Tao, A. P. Khain, J. Simpson, D. E. Johnson, 2009: Sensitivity of a cloud-resolving model to bulk and explicit bin microphysical schemes. Part II: Cloud microphysics and storm dynamics interactions. *Journal of Atmospheric Sciences*, **66**, 22-40.

**Contributors:** Chuntao Liu (University of Utah) and Hirohiko Masunaga (Nagoya University, Japan)

**Data Sources:** 9-year TRMM observations of squall lines over central US; C-band ground radar observations; GCE cloud-resolving simulations.

#### Technical Description of Figures:

**Figure 1:** Simulated radar reflectivities and brightness temperatures are calculated using our recently developed Satellite Data Simulator Unit (SDSU). Particle size distributions simulated by GCE model are used as input for SDSU. C-band surface radar reflectivities are taken from the same case. The TRMM satellite does not have any observations for this case. To utilize long-term TRMM satellite observations, we chose to compare only the stratiform region of the squall line, where the structures are uniform, even for different cases. All squall lines from May to July are visually identified from the 9-year TRMM database, and their composites are used for comparisons. As shown in Figure 1, TRMM PR CFADs show very small variations, even for the 18 case composite. The second row in Figure 1 shows that the initial simulation produced much higher radar reflectivity, especially from 4 km to 8 km, compared with both C-band and TRMM PR observations. By introducing stronger temperature dependency of the collection efficiency in the bin microphysical scheme, we were able to improve the simulated radar reflectivity, producing a better match to the TRMM observations (the third row). The probability distribution functions and mean TMI brightness temperatures shown in the third column also compare well with observations.

**Scientific significance:** The Goddard Spectral Bin Microphysical Scheme is the current state-of-the-science in bin microphysics. It explicitly simulates the evolution of cloud hydrometeors (raindrops, pristine ice, snow, graupel, hail) using 33 mass bins for each species. The GCE model has one such scheme successfully implemented. Massively parallel computing resources at NASA (GSFC and Ames) permit more realistic cloud system simulations using this computationally expensive and sophisticated microphysical scheme. However, careful validation is critical. This study shows how long-term satellite observations can be used to test and improve microphysical processes in a cloud model.

**Relevance for future science and relationship to Decadal Survey:** The Goddard Spectral Bin Microphysical Scheme will be applied in both scientific study and algorithm development for future satellite missions. For example, it is used to test future GPM algorithms with its unique data of simulated particle size distributions, shapes, and densities. Databases constructed from GCE model simulations are also the backbone of TRMM latent heating retrieval algorithms. Because clouds are a significant uncertainty in current global simulations and future climate change studies, cloud-resolving models using bin microphysics like GCE can contribute to improved global simulations, both directly through global cloud-resolving simulations and multi-scale modeling frameworks, and indirectly through process understandings, offering insights to cumulus parameterization schemes in GCMs.



# Recent trends of tropical hydrological cycle inferred from GPCP and ISCCP data

Yaping Zhou (Code 613, USRA-MSU)

Among the greenhouse gas-induced climate change projections, tropical hydrological cycle changes can be expected to cause shortage or excess of precipitation in many regions, and that in turn would impact all life on Earth. We have examined decadal trends of the tropical hydrological cycle in the GPCP precipitation and ISCCP cloud and radiation data to determine if such trends can provide an observation-based benchmark for model predictions of the ongoing climate change. The results show (1) intensification of tropical precipitation in the rising regions of the Walker and Hadley circulations and weakening over the sinking regions – showcasing the “wet-getting-wetter, dry-getting-drier” phenomena; (2) poleward shift of the subtropical dry zones (up to  $2^{\circ}$  decade $^{-1}$  in June-July-August (JJA) in the Northern Hemisphere and  $0.3$ – $0.7^{\circ}$  decade $^{-1}$  in JJA and September-October-November (SON) in the Southern Hemisphere consistent with an overall broadening of the Hadley circulation; and (3) significant poleward migration of cloud boundaries of Hadley cell and plausible narrowing of the high cloudiness in the Intertropical Convergence Zone (ITCZ) region in some seasons. These trends indicate a strengthening of the tropical hydrological cycle with intensification of extremes of dry and wet conditions.

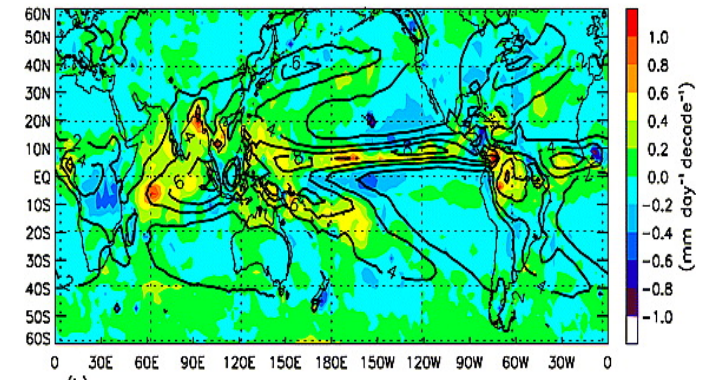


**Figure 1:** GPCP climatology (contour) and linear trends (shading) indicate that precipitation increases at climatologically wet regions and decreases at climatologically dry regions.

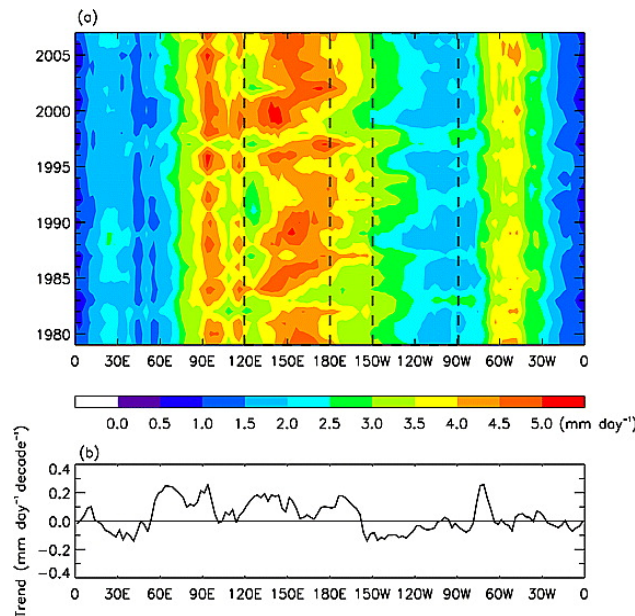
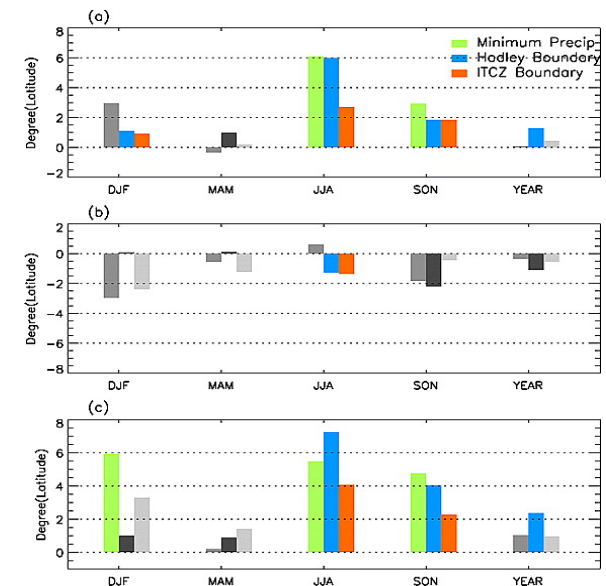


**Figure 2 (left):** Time-longitude distribution of meridionally averaged ( $30^{\circ}\text{S}$ – $30^{\circ}\text{N}$ ) GPCP annual mean precipitation (a) and corresponding linear trend with longitude (b) show that the rising (sinking) areas of the Pacific Walker circulation are represented with positive (negative) precipitation trends.

**Figure 3 (right):** Linear trends of the latitude of minimum precipitation, ITCZ, and Hadley cell boundaries inferred from GPCP for each season and the year for the Northern Hemisphere (a) and the Southern Hemisphere (b) show poleward shifts of the Hadley cell and subtropical dry zones. Total expansion of the tropics in these three indices are shown in (c). For quantities significant at the 90% level, bars are shaded green, blue, and orange, respectively.





Name: Yaping Zhou, Code 613  
E-mail: Yaping.Zhou-1@nasa.gov  
Phone: 301-614-6235

### References:

Zhou, Y. P., K.-M. Xu, Y. C. Sud, and A. K. Betts (2011), Recent trends of the tropical hydrological cycle inferred from Global Precipitation Climatology Project and International Satellite Cloud Climatology Project data, *Journal of Geophysical Research - Atmospheres*, doi:10.1029/2010JD015197.

**Data Sources:** The Global Precipitation Climatology Project (GPCP) monthly precipitation data and the International Satellite Cloud Climatology Project (ISCCP) FD products

### Technical Description of Figures:

**Figure 1:** GPCP climatology and linear trends show that the majority of the tropical areas exhibit trends of increasing precipitation; the strongest positive trends are seen in the heavy precipitation areas (i.e., Intertropical Convergence Zone (ITCZ), South Pacific Convergence Zone (SPCZ), Indian Pacific warm pool, and the Amazon regions), while the strongest negative trends are noted over the light precipitation area (i.e., at both edges of the ITCZ, south of equatorial Africa). This figure well illustrates that wet (dry) regions tend to become wetter (drier).

**Figure 2:** (a) Heavy precipitation is located over the rising branches of the Pacific and Indian Walker circulations in the 90–180°E region. Relatively heavy precipitation is also found over the Atlantic Ocean in the 40–70°W region corresponds to the rising branch of the Atlantic Walker circulation. Light precipitation is found in the sinking branches of the three Walker circulations and continental Africa. (b) Zonal distribution of the trends shows positive trends over the rising regions of the three Walker circulations, and negative trends over the regions of light precipitation.

**Figure 3:** This plot summarizes trends (or total migration) of the Hadley cell and ITCZ boundaries as well as the position of minimum precipitation. In the Northern Hemisphere, the trends of Hadley cell and ITCZ boundaries reveal a significant northward migration in all the seasons except MAM, accompanied by a significant northward shift of the minimum precipitation. In the Southern Hemisphere, the Hadley cell and ITCZ also migrates poleward, but with much smaller magnitude. The tropical regions have expanded in each of the four seasons, but significant trends are found in JJA and SON only.

**Scientific significance:** Among the greenhouse gas-induced climate change projections, tropical hydrological cycle changes can be expected to cause shortage or excess of precipitation in many regions and that in turn would impact all life on Earth. We have examined decadal trends of the tropical hydrological cycle in the GPCP precipitation and ISCCP cloud and radiation data to determine if such trends can provide an observation-based benchmark for model predictions of the ongoing climate change. The GPCP precipitation data revealed intensification of tropical precipitation in the rising regions of the Walker and Hadley circulations and weakening over the sinking regions. The study also confirms broadening of Hadley cell in recent decades in precipitation and related cloud and radiation fields. These trends indicate a strengthening of the tropical hydrological cycle with intensification of extremes of dry and wet conditions.

**Relevance for future science and relationship to Decadal Survey:** This research is directly relevant to two of NASA's Earth Science focus areas: water and energy cycle and climate variability and climate change. We have demonstrated intimate connections between atmospheric latent heating and radiative heating through dynamical cloud-precipitation system. Detection of climate change demands monitoring all aspects of the climate system (clouds, precipitation, radiation, atmosphere and land surface moisture, etc) with extended duration in order to get a consistent picture.





# Global Total Ozone Impacts Due to Greenhouse Gases and Chlorine- and Bromine-Containing Compounds, 1850-2100



Eric Fleming (Code 614, NASA GSFC and SSAI)

Charles Jackman (Code 614, NASA GSFC)

Stratospheric ozone is strongly impacted by the greenhouse gases (GHGs)  $\text{CO}_2$ ,  $\text{CH}_4$ , and  $\text{N}_2\text{O}$ , and man-made ozone depleting substances (ODSs) containing chlorine (Cl) and bromine (Br).

Figure 1 shows that the Cl+Br (from ODSs) and the GHGs have undergone substantial past increases. While the Cl+Br are expected to diminish through the 21<sup>st</sup> century, the GHGs are projected to strongly increase based on the Intergovernmental Panel on Climate Change (IPCC) medium (A1B) scenario.

We use a model of atmospheric chemistry and transport to illustrate the individual impacts on global ozone for 1850-2100 due to the GHGs and the Cl+Br (Figure 2).  $\text{N}_2\text{O}$  and Cl+Br lead to ozone depletion, while  $\text{CO}_2$  and  $\text{CH}_4$  increase ozone.

Figure 2 also shows these impacts in a historical context, and reveals that all changes were relatively small prior to 1960. Substantial ozone depletion by Cl+Br from the ODSs occurred after 1960 (blue line), which is also reflected in the observations (“+” signs). By 2100, the GHGs are projected to have a substantial effect on ozone, with  $\text{CO}_2$  having the largest individual impact. The full model simulation (black line) shows that the net result of increasing GHGs and diminishing Cl+Br will be 1.5% *more* ozone in 2100 compared to 1850 and 1950.

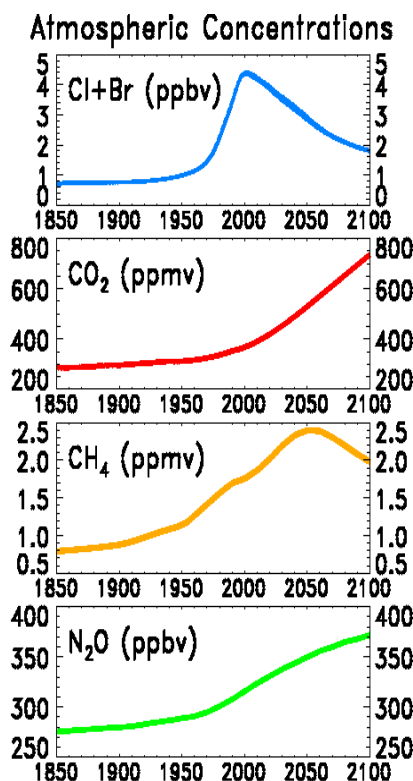


**Figure 1.** Time lines for 1850-2100 of the atmospheric concentrations of: Cl+Br from ODSs (top);  $\text{CO}_2$  (middle top);  $\text{CH}_4$  (middle bottom); and  $\text{N}_2\text{O}$  (bottom). Values are in parts per million by volume (ppmv) or parts per billion by volume (ppbv).

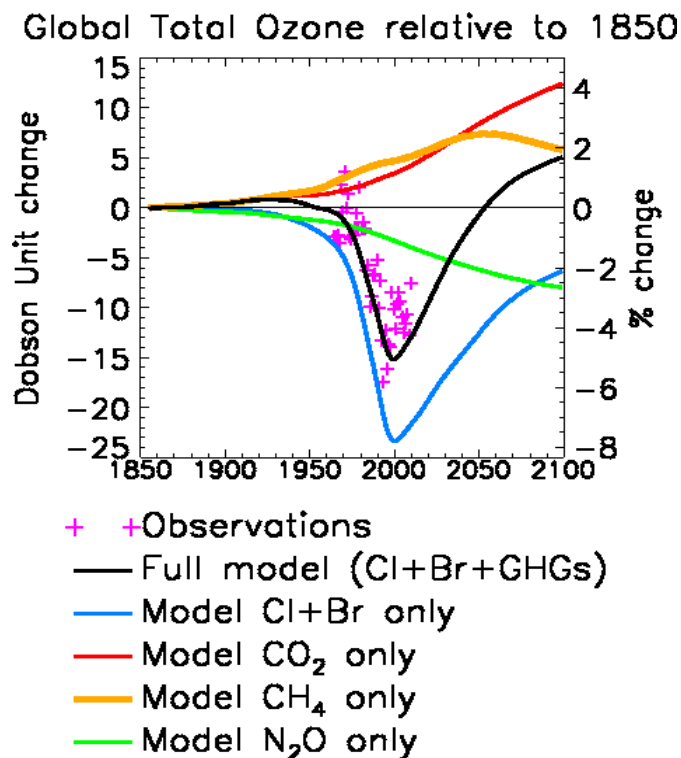


**Figure 2.** Time lines for 1850-2100 of global total column ozone, relative to 1850, from observations (“+” signs) and five model simulations using the following inputs: Cl- and Br-containing ODSs only (blue line);  $\text{CO}_2$  only (red line);  $\text{CH}_4$  only (orange line);  $\text{N}_2\text{O}$  only (green line); and the full model with all GHGs and ODSs inputs combined (black line). Values are expressed in Dobson unit change (left axis) and percentage change (right axis).



Name: Eric Fleming, SSAI, NASA GSFC, Code 614  
E-mail: eric.l.fleming@nasa.gov  
Phone: 301-614-5983



### References:

Fleming, E. L., C. H. Jackman, R. S. Stolarski, and A. R. Douglass, A model study of the impact of source gas changes on the stratosphere for 1850-2100, *Atmospheric Chemistry and Physics*, 11, 8515-8541, 2011.

**Data Sources:** Total column ozone observations updated from the paper by V.E. Fioletov et al., Global ozone and zonal total ozone variations estimated from ground-based and satellite measurements: 1964-2000, *Journal of Geophysical Research*, 107 (D22), 4647, doi:10.1029/2001JD001350, 2002. These comparisons included the long record of NASA Total Ozone Monitoring Spectrometer (TOMS) data.

**Technical Description of Figures:** Figure 1 shows that the atmospheric concentrations of chlorine+bromine had only small increases from 1850 through ~1960, but then increased rapidly and peaked in year 2000. They are projected to gradually diminish through the 21<sup>st</sup> century. The GHGs similarly increased relatively slowly before ~1960, but are projected to have significant increases through the 21<sup>st</sup> century, based on the IPCC medium (A1B) scenario. Figure 2 shows model simulations with the ozone impacts due to chlorine+bromine and the GHGs varied individually (colored lines). The full model includes the ODSs and GHGs varied altogether (black line), and represents the combined contribution of these compounds to long-term ozone changes. This simulation agrees well with the rate of decrease in ozone seen in the observations from the ~1960s to 2000.

**Scientific significance:** Stratospheric ozone is important because it shields the Earth's surface from harmful ultraviolet radiation from the sun. Man-made ozone depleting substances, including chlorofluorocarbons (CFCs) and halons contain chlorine and bromine which destroy ozone. These substances were first developed in 1900, became widely used in the 1970s through the early 1990s, but have now been regulated under international agreements. As a result, atmospheric chlorine and bromine reached peak concentrations in 2000, and have been slowly decreasing over the past decade. This decrease is expected to continue through out the 21<sup>st</sup> century. Ozone is also affected by the greenhouse gases CO<sub>2</sub>, CH<sub>4</sub>, and N<sub>2</sub>O. These have both natural and man-made sources, the latter of which have been increasing since the 1800s and are expected to continue into the future. CO<sub>2</sub> and CH<sub>4</sub> loading lead to ozone increases; N<sub>2</sub>O leads to ozone decreases.

Simulations with the GSFC two-dimensional model illustrate the individual long-term impacts of CO<sub>2</sub>, CH<sub>4</sub>, N<sub>2</sub>O, and the ODSs on global total column ozone. These simulations (Figure 2) indicate that all four perturbations will have substantial impacts on ozone during the 21<sup>st</sup> century, with changes of -2 to +4% by 2100, relative to 1850. CO<sub>2</sub> loading, which cools the stratosphere and reduces the ozone chemical loss rates, has the largest individual effect, causing a 4% increase over the 1850-2100 time period. The combined impact of all perturbations results in ozone amounts that are 1.5% larger in 2100 compared to 1850 and 1950. This has important implications for global climate and surface UV. The simulations also indicate that prior to the widespread use of ODSs during the late 20<sup>th</sup> century, ozone increased slightly from 1850 to a broad maximum during the 1920s-1930s (a 0.3% increase from 1850). This was caused by the CO<sub>2</sub>- and CH<sub>4</sub>-induced ozone increases which outpaced the ozone losses caused by the small ODS and N<sub>2</sub>O loading during this time. These simulations therefore help to better quantify the man-made impacts on ozone, both in a historical context and in future projections.

**Relevance for future science and relationship to Decadal Survey:** This work shows the importance of man-made compounds in controlling the past and future changes in ozone. It will be important to carry out further measurements of ozone and related constituents (e.g., chlorine-, bromine-, and nitrogen-containing compounds) to better understand future ozone variations. Thus, measurements of the proposed Decadal Survey's Global Atmospheric Composition Mission (GACM) are necessary to continue investigations of long-term ozone changes.